Effect of edge transmission and elastic scattering on the resistance of magnetic barriers: Experiment and theory

M. Cerchez, S. Hugger, and T. Heinzel*
Heinrich-Heine-Universität, Universitätsstrasse 1, 40225 Düsseldorf, Germany

N. Schulz
Fraunhofer Institut für Angewandte Festkörperphysik, Tullastrasse 72, 79108 Freiburg, Germany
(Received 26 October 2006; published 31 January 2007)

Strong magnetic barriers are defined in two-dimensional electron gases by magnetizing dysprosium ferromagnetic platelets on top of a Ga[Al]As heterostructure. A small resistance across the barrier is observed even deep inside the closed regime. We have used semiclassical simulations to explain this behavior quantitatively in terms of a combined effect of elastic electron scattering inside the barrier region and $E\times B$ drift at the intersection of the magnetic barrier with the edge of the Hall bar.

DOI: 10.1103/PhysRevB.75.035341 PACS number(s): 73.23.−b, 75.70.Cn

I. INTRODUCTION

A two-dimensional electron gas (2DEG) reacts sensitively to perpendicular magnetic fields. Making the magnetic field inhomogeneous opens the door to a wide variety of fascinating effects and applications, ranging from magnetic superlattices[1] and magnetic waveguides[2] to Hall sensors for magnetic nanostructures.[3,4] One particularly simple magnetic field structure is the *magnetic barrier*, namely a perpendicular magnetic field configuration strongly localized along one in-plane direction and homogeneous in the second one.[5,6] In a classical picture, magnetic barriers can be considered as selective transmitters that filter the electrons according to their angle of incidence.[5] In a ballistic sample without edges, one would therefore expect that above a critical barrier height the barrier *closes*, all electrons are reflected and the resistance approaches infinity. Recently, magnetic barriers have received renewed interest due to their potential applications as tunable spin filters and detectors, both of which are highly desirable spintronics devices.[7–15] These theoretical works suggest that a high degree of spin polarization may be achievable with magnetic barriers in suitable materials.

Considering the elementary character and the simplicity of a magnetic barrier, it is surprising that only a few transport experiments on such structures have been reported. In Ref. 16 a magnetic barrier with a square profile has been experimentally realized in a highly sophisticated sample, namely a 2DEG containing a graded step. It was observed that even for strong magnetic fields, the barrier resistance remains finite. The results of these experiments have been subsequently interpreted within a classical model,[17] which shows that $E\times B$ drift effects at the edge of the 2DEG, as well as elastic scattering, limit the resistance to finite values.

In all other experiments reported so far except Ref. 16, the magnetic barrier has been generated in conventional Ga[Al]As heterostructures by magnetizing a ferromagnetic platelet, located on top of the sample, by an in-plane magnetic field.[18–23] In such a setup, the magnetic barrier originates from the z component of the stray field of the ferromagnet, see Fig. 1. This experimental implementation is also the basis for a significant fraction of the theoretical studies.[14,15,24,25]

For an experimental implementation of the theoretical concepts, a detailed and quantitative understanding of the measured transmission properties of tunable magnetic barriers is needed. Previous studies have already shown that both edge transmission and scattering in the barrier region are relevant.[21,23] Here, we build on these results and discuss in detail how the resistance of tunable magnetic barriers depends upon the $E\times B$ drift at the edges, on the elastic scat-

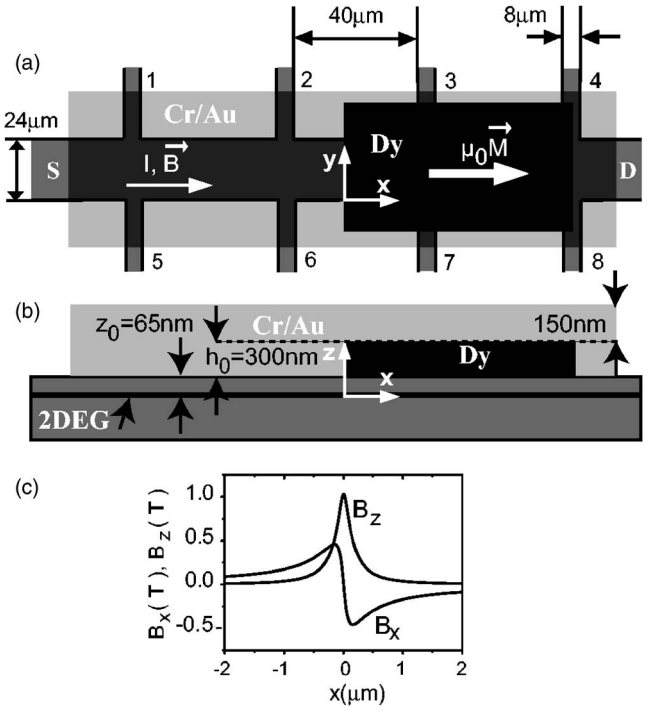

FIG. 1. (a) Top view of the sample: a dysprosium platelet is placed on top of a Hall bar with source and drain contacts (left and right) and voltage probes 1 to 8. The structure is covered by a homogeneous Cr/Au gate. The parallel magnetic field is applied in the x direction. (b) Cross section of the sample in the x-z plane. (c) At the edges of the Dy film, the fringe field in the z direction $B_z(x)$ is highly localized in the x direction. Also shown is the x component of the fringe field.

tering and on thermal smearing. In order to magnify these influences, we have prepared our ferromagnetic films from dysprosium which has a particularly large bulk saturation magnetization of $\mu_0 M = 3.75$ T.[26,27] This allows us to drive the barriers well into the closed regime, where the transport through the structure is exclusively determined by the effects of interest here. In addition, a top gate was used to tune the electron density.

These measurements are interpreted in a semiclassical picture based on the billiard model for ballistic conductors.[28,29] We find that (i) the combination of both $E \times B$ type edge drifts and elastic scattering in the barrier determines the barrier resistance, (ii) reasonable assumptions regarding the distribution of scattering angles for the elastic electron scattering lead to excellent agreement of the experimental data with the model, and (iii) thermal smearing has a marginal influence at liquid helium temperatures.

The outline of the paper is as follows: in Sec. II, we describe the sample preparation, the experimental setup and the measurement methodology. The experimental results are presented in Sec. III, while the semiclassical model and its application to our measurements is the topic of Sec. IV. The paper concludes with a summary and a discussion (Sec. V).

II. SAMPLE PREPARATION AND EXPERIMENTAL SETUP

A commercially available GaAs/$Al_xGa_{1-x}As$ heterostructure[30] with a 2DEG 65 nm below the surface was laterally patterned by using optical lithography and subsequent processing steps. A Hall bar geometry (Fig. 1) was defined by wet chemical etching. Au/Ge ohmic contacts were defined at source and drain contacts and at the voltage probes 1 to 8. A dysprosium (Dy) platelet with a thickness of $h_0 = 300$ nm was defined at the heterostructure surface by Dy thermal evaporation at a base pressure of 2×10^{-6} mbar. A Cr/Au gate layer of 150 nm thickness was deposited on top to prevent the Dy from oxidizing under ambient conditions and to allow the carrier density to be tuned. Six samples were measured, and all showed qualitatively identical behavior. Here, we discuss data taken from one representative sample.

The samples were inserted in a liquid helium cryostat with a variable temperature insert that permits variation of the temperature between 2 K and room temperature. The sample stage is equipped with a rotatable sample holder, such that the magnetic field could be oriented within the x-z plane with an accuracy better than 0.1 degrees.

The carrier densities and the electron mobility were determined from conventional four-probe measurements of the components of the resistance tensor, R_{xx} and R_{xy} in perpendicular magnetic fields. The ungated electron density is 2.3×10^{15} m^{-2}, and the mobility at a temperature of 2 K is 29.0 m^2/V s, corresponding to a Drude scattering time of $\tau_D = 10.2$ ps and an elastic mean free path of 2.2 μm. The quantum scattering time was determined from the envelope of the Shubnikov-de Haas oscillations[31] as $\tau_q = 1.05$ ps. The vanishing of the Hall voltage was furthermore used to detect the parallel magnetic field configuration. At the maximum magnetic field B of 8 T used in our experiments, we estimate that the maximum external perpendicular magnetic field component is below 5 mT.

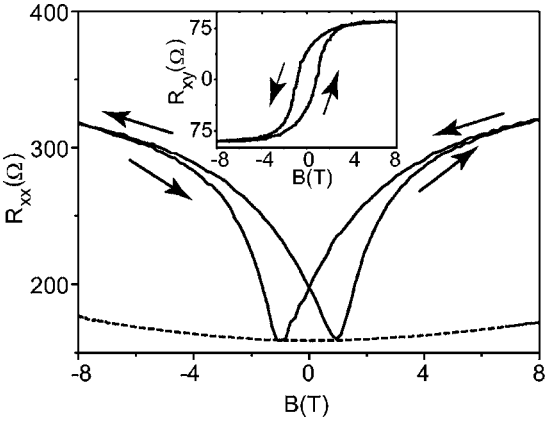

FIG. 2. Resistance of the magnetic barrier as a function of the magnetic field (full lines), as measured between contacts 2 and 3. The dashed line shows the magnetoresistance of the 2DEG, measured between contacts 1 and 2. Inset: Hall resistance of the magnetic barrier (the voltage was collected between contacts 4 and 8). The arrows denote the scan directions.

Strong parallel magnetic fields are well known to affect the transport properties of 2DEGs by modifying the density of states and the interactions.[32] In addition, the electron effective mass becomes slightly anisotropic.[33] These effects show up as a weak and approximately parabolic magnetoresistivity.

Increasing B also magnetizes the Dy film along the x direction. The z component of the fringe field at the 2DEG is strongly localized at the edge of the Dy in the x direction and forms the magnetic barrier.[18,34] The x and z components of the fringe field are shown in Fig. 1(c) for the literature value of the saturation magnetization of Dy. Assuming that the fringe field follows the corresponding analytic expressions,[17,20] $B_z(B,x)$ is given by

$$B_z(B,x) = -\frac{\mu_0 M(B)}{4\pi} \ln\left(\frac{x^2 + z_0^2}{x^2 + (z_0 + h_0)^2}\right), \qquad (1)$$

where z_0 is the distance of the 2DEG from the surface and h_0 denotes the thickness of the Dy film, see Fig. 1(c). This relation neglects the second magnetic barrier residing at contacts 4 and 8, which is justified since it is sufficiently far away from the region probed between contacts 2 and 3. Edge roughness of the magnetic film may also lead to deviations from Eq. (1). We characterized the Dy edge by atomic force microscope measurements and found an edge roughness (single standard deviation) of 35 nm, which is smeared out to a large extent at the 2DEG. We therefore neglect the edge roughness in the following. The magnetization in the x direction as a function of B is denoted by $M(B)$, which can be estimated from Hall measurements on a magnetic barrier[18] as described below. The x component of the fringe field has a much smaller effect on the 2DEG and is moreover small compared with the B field required to establish saturation (i.e., $B_{sat} \approx 4.5$ T, see the inset in Fig. 2). It is therefore ne-

glected in the following.

A current of 100 nA at a frequency of 13.6 Hz is passed from source to drain. The barrier resistance is obtained from the voltage measured between contacts 2 and 3 (Fig. 1) with a lock-in amplifier. The Hall voltage measured between contacts 4 and 8 is used to determine $M(B)$. We assume in the discussion below that the magnetic barriers at both edges of the Dy platelet differ only by their sign.

III. EXPERIMENTAL RESULTS

Figure 2 shows a typical magnetoresistance trace $R_{xx}(B)$ of our samples, measured on sample A. The traces are hysteretic, reflecting the magnetization characteristics of the Dy film (inset). At the coercive magnetic fields at ±0.9 T, $R_{xx}(B)$ has minima which equal to high accuracy the magnetoresistance outside the Dy film measured over an identical distance. This shows that the micromagnetic structure in the Dy film which becomes most relevant around the coercive magnetic field[20] has no noticeable effect in our experiments. $R_{xx}(B)$ increases as one goes away from the coercive field, but neither saturates nor approaches infinity, even well above the saturation magnetic field. The slope dR_{xx}/dB above B_{sat} is only partly due to the parabolic background. As discussed in more detail below, if our barrier were fully ballistic and without edges, it would close at $B=0.7$ T away from the minimum of R_{xx}. Thus, in 88% of the magnetic field interval scanned, the transmission is governed by the edge and scattering effects of interest. Note that the $R_{xx}(B)$ traces are slightly asymmetric around their minimum. We attribute this effect to the proximity of the voltage probes (17 μm) to the magnetic barrier, over which the electrons ejected from the barrier may not yet form a Fermi sphere, even though the probes are about eight elastic mean free paths away from the barrier. Similar effects have been observed by Leadbeater *et al.*[16] and subsequently been explained in detail by Ibrahim *et al.*[17]

The Hall resistance of the magnetic barrier (inset in Fig. 1) measures $B_z(B,x)$, averaged over the spatial extension L in the x direction of the Hall probe contacts 4 and 8, i.e., over 8 μm, according to

$$R_{xy}(B) = -\frac{\alpha}{Lne}\int_{-L/2}^{L/2} B_z(B,x)dx. \qquad (2)$$

Here, α represents a Hall factor which may deviate from 1, depending on the sample geometry and the mean free path.[35–37] For our structure, $\alpha \approx 1$ is expected,[3] and we have no reason to assume otherwise, in contrast to the findings reported in Ref. 20. Here, we have assumed that the magnetic barrier on top of our Hall cross is adequately described by the ballistic model, even though the mean free path is smaller than the width of the voltage probes. Since, however, the FWHM of our barrier in the closed regime is no larger than 300 nm and thus much smaller than the mean free path, and the maximum magnetic field multiplied by the electron mobility $B_{\max} \times \mu \gg 1$ for our system in the closed regime, the diffusive model developed in Ref. 38 does not strictly apply as well,[36] while to the best of our knowledge, a model

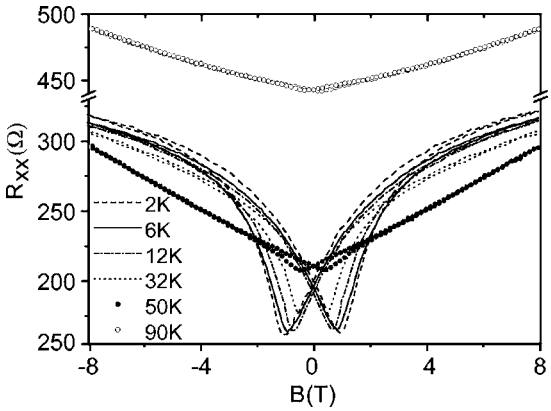

FIG. 3. Temperature dependence of the magnetic barrier magnetoresistance.

for the intermediate regime is not available. For $\alpha=1$, we determine from the measured $R_{xy}(B)$ a saturation magnetization of $M_s=1.9$ T for our Dy films. This is significantly below the literature value for bulk dysprosium. We attribute this reduction to the embedding of oxygen into the Dy film during metallization, as well as to the granularity of the film.[27] This interpretation is supported by our observation of $\mu_0 M_s$ dropping over time in samples where the Dy films is not covered by a Cr/Au layer.

Figure 3 reproduces the behavior of the barrier magnetoresistance as the temperature is changed. As the temperature is increased, the magnetic barrier resistance is reduced. At the same time, the shape of the barrier becomes more nearly triangular and the hysteresis decreases. Simultaneously, the resistance minima increase and are shifted to smaller absolute values of B. As will be explained in more detail below, this behavior can be understood in terms of a combination of increased scattering and a reduced coercivity of the Dy film as the temperature is increased, while the thermal smearing of the Fermi function plays a marginal role. A slight hysteresis is observed even above the literature value for the Curie temperature of bulk Dy, $T_C=85$ K.[26] The enhancement of the Curie temperature is a second indication of crystal imperfections in our Dy films.[27]

IV. SIMULATION AND INTERPRETATION OF THE EXPERIMENTS

Our numerical approximation of the magnetic barrier resistance is exemplified using the data of Fig. 2. The analysis is based upon the billiard model for quasiballistic conductors[29] and the Landauer-Büttiker formalism.[28] Electrons are injected into the barrier region starting from a fixed x position 10 μm to the left of the barrier at random positions in the y direction across the Hall bar of width $W=24$ μm. They start out with the Fermi velocity, while their directions are arbitrarily distributed over all angles with positive x component. We solve the differential equations describing the classical motion of the electrons to obtain their trajectories until either it is rejected by the barrier and passes the starting line in the opposite direction, or until it travels through the barrier and reaches the x position 10 μm to its

right. At this distance, $B_z(x)$ is negligible. Injecting the electrons at larger distances does not modify the results. The edges of the Hall bar have been incorporated by constant, reflective electric fields in the regions $|y|>12$ μm. Strong electric edge fields generate specular reflection. The magnetic barrier is incorporated as given by Eq. (1) in the x direction and homogeneous in the y direction. We have introduced scattering in the 2DEG by assuming scattering after time of flights which obey a Poisson distribution with a time constant of τ_q. The electrons in a 2DEG in a modulation-doped Ga[Al]As heterostructure are predominantly scattered at the ionized donors in the doping layer, and the corresponding *screened Coulomb scattering* is known to form an approximately Gaussian distribution of scattering angles.[39] We therefore assume a Gaussian distribution of scattering angles θ with a standard deviation of 0.1π, centered at $\theta=0$ and limited to $|\theta|\leqslant\pi$. Within our model, the times of flight between two subsequent scattering events form a Poisson distribution with an expectation value of τ. At a scattering event, the angles between the initial and the final electron velocity vector direction are changed according to the distribution function described above. These two distributions reproduce the experimentally determined values for τ_q and τ_D.

We remark that our simulation results are rather insensitive to the chosen distribution function of scattering angles. We have also used a rectangular distribution, namely a constant probability for scattering angles $\theta\leqslant 0.06\pi$ and a probability of zero for larger angles. Even though we find slightly higher values for the resistance (about 2.5%) at small fields, the same values are found in the closed regime.

For each magnetic field, 40 000 electrons of Fermi energy E_F are injected. The transmission is determined by

$$T(E_F,B)=\frac{1}{2W}\int_{-W/2}^{W/2}dy\int_{-\pi/2}^{\pi/2}\cos(\alpha)t(E_F,\alpha,y,B)d\alpha. \quad (3)$$

Here, α is the angle between the x direction and the direction in which the electron is injected and $t(E_F,\alpha,y,B)$ is either 1 or 0 depending on whether the electron with the corresponding initial conditions is transmitted or not. We note that the carrier density under the Dy film may differ from that underneath the Cr/Au gate, as a consequence of different Schottky barriers. Hall measurements at voltage probes 1 and 5, as well as at 3 and 7, respectively, indicate that the electron density under the Dy is roughly 5% larger as compared with the density measured outside, but this value is ambiguous since the z component of the Dy fringe field superimposes on the homogeneous magnetic field in the z direction and we were unable to separate these two contributions to the modified Hall resistance.[20] We have neglected this density step in our simulations.

The conductance is given by

$$G(E_F,B)=N(E_F)\frac{2e^2}{h}\frac{T(E_F,B)}{1-T(E_F,B)}, \quad (4)$$

where $N=2W/\lambda_F=918$ is the number of modes in our Hall bar and λ_F is the Fermi wavelength. We note that according to Eq. (4), the contact resistance ($R_c=h/2e^2N=14.1$ Ω) between an infinitely extended 2DEG and the Hall bar does not contribute to R_{xx}.[20,29] From Eq. (4), the longitudinal resistance R_{xx} across the barrier for a given carrier density is readily obtained from $R_{xx}(B)\equiv 1/G(E_F,B)$. As a test simulation, we have turned off all scattering and set the electric field at the edges to zero, thereby simulating a ballistic magnetic barrier which extends to infinity in the y direction. In this case, the numerical results closely match the corresponding analytical expression[21] and reproduce the critical angle of incidence for which the magnetic barrier closes to an accuracy of 1 degree.

For a comparison of the simulations with the experiments, the magnetization trace $M(B)$ shown in the inset of Fig. 2 is used to map the height of the magnetic barrier onto the experimental value of B. Results of the simulations are represented in Fig. 4(a). Most significantly, the addition of the edge electric fields to the ballistic system limits the resis-

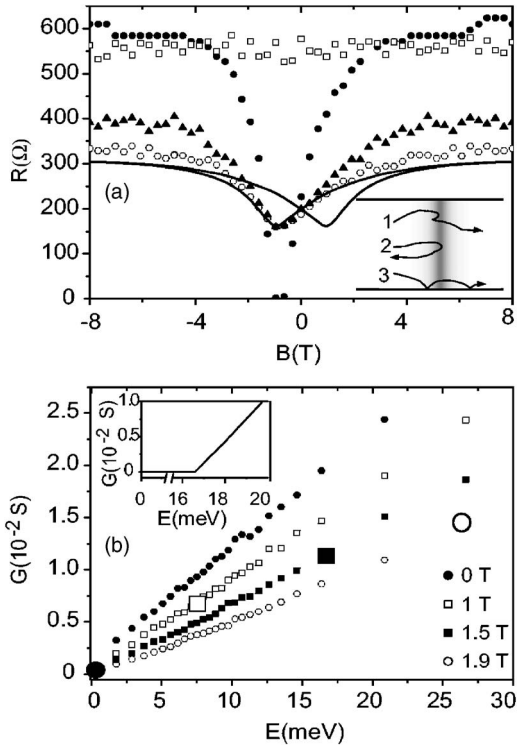

FIG. 4. (a) Comparison of model calculations for $R_{xx}(B)$ with the experimental trace of Fig. 2 (full line), corrected for the magnetoresistivity of the 2DEG which is set to its constant value at $B=0$ T. Full circles, R_{xx} for a barrier with edges (edge electric field $|\vec{E}|=10^6$ V/m) and no scattering; triangles, R_{xx} for the barrier with no edges but scattering according to the experimentally determined scattering times; open circles, barrier resistance with both scattering and edge electric field; open squares, R_{xx} for the structure with edges and a small quantum scattering time of $\tau_q=0.2$ ps. Inset, typical calculated trajectories in the closed regime: scattering inside the magnetic barrier (trace 1) as well as $E\times B$, drifts by edge electric fields (trace 3) are responsible for a finite resistance. (b) Conductance of the magnetic barrier as a function of electron energy for several values of $\mu_0 M$ including edges and scattering. Large symbols in the figure correspond to the critical energy for which an infinitely extended barrier in a ballistic system will close (the corresponding energy dependent conductance for $\mu_0 M=1.5$ T is shown in the inset).

tance in the closed regime to finite values. Some electrons that would be reflected at the barrier away from the edges are pulled through the barrier at the edges due to the $E \times B$ drift, see the inset in Fig. 4(a). This effect is the sole reason for a finite resistance in the closed regime, as long as scattering is disregarded. The barrier resistance decreases as the edge electric field is increased. In our simulations, we have assumed an electric field of $|\vec{E}|=10^6$ V/m. This value can be considered an upper limit, based upon measurements of the steepness of the confining walls[40] and in agreement with the consideration that a potential change of the order of E_F/e cannot occur over a length smaller than the screening length.[41] We note that the simulated barrier resistance is only weakly dependent on the strength of the edge electric field.

For an infinitely extended closed magnetic barrier in a disordered system, the resistance is also kept finite by scattering events in the barrier region, see Fig. 4(a). This is again illustrated by the characteristic trajectories, see the inset in Fig. 4(a): a scattering event may redirect an electron which in the absence of scattering would be rejected by the barrier. For elastic mean free paths comparable to or below the spatial extension of the barrier, the barrier becomes unimportant [open squares in Fig. 4(a), where the simulated elastic mean free path was 440 nm].

In comparison with the experimental data in Fig. 2(a), we observe that the numerical trace for $R_{xx}(B)$ that takes only the scattering into account but disregards edge effects disagrees significantly with the experiment. Here, the measured background magnetoresistance (Fig. 2) has been replaced by its value at $B=0$ T. The shape of the measurement trace is reproduced, but its absolute value differs by up to 30%. We point out that in this simulation, the only adjustable parameter is the distribution of scattering angles under the constraints set by the measured values for τ_D and τ_q, which is determined by the details of the disorder potential landscape.

From this separate discussion of the two mechanisms, it emerges that a combination of both edge transmission and scattering-induced transmission determines $R_{xx}(B)$. In fact, inclusion of both elastic scattering in accordance with the measured scattering times, as well as an electrostatic edge field of $|\vec{E}|=10^6$ V/m, gives a very good reproduction of the measured trace, see Fig. 4(a). We refrain from fitting the experimental data since further uncertainties may have an influence on this level of accuracy. First, there is a slight asymmetry of the measured traces, which we attribute to asymmetries in the voltage probe geometry.[17] Second, the shape of the magnetic barrier may deviate from Eq. (1), and it may be inhomogeneous in the y direction. Furthermore, the electron density below the Dy deviates from that below the Cr. This effect could in principle be avoided by preparing a thin, homogeneous metal electrode between the semiconductor surface and the ferromagnet.

In order to investigate the influence of thermal smearing, we have calculated the energy dependent conductance $G(E,B)$ by varying the energy in Eq. (4), from which the conductance at nonzero temperatures is obtained via

$$G(B,T) = \int_0^\infty G(E,B)\left(-\frac{\partial f}{\partial E}\right)dE, \tag{5}$$

where f denotes the Fermi-Dirac distribution function. Figure 4(b) shows that the simulated $G(E,B)$ is a nearly linear function of the electron energy. According to Eq. (5), $G(B,T)$ becomes independent of temperature for $G(E,B) \propto E$. A similar relation is also approximately found within an analytic treatment of the infinitely extended, open magnetic barrier in a ballistic 2DEG,[21] see the inset in Fig. 4(b). Hence, the inclusion of both edge effects and scattering does not change this insensitivity of the magnetic barrier resistance to thermal smearing. We conclude, therefore, that the changes of $R_{xx}(B)$ with temperature are, besides the temperature dependence of $\mu_0 M(B)$, mainly due to the temperature dependence of the scattering times. In our experiments, we find that both scattering times are constant up to 6 K, and in addition, we do not see significant changes in $R_{xx}(B)$, see Fig. 3, while for larger temperatures, the observed Shubnikov-de Haas oscillations no longer allow a meaningful determination of τ_q. Hence, a reasonable approximation of the measurements at higher temperatures requires more detailed information regarding the scattering times and the distribution of scattering angles than available from our experiments.

We have furthermore studied numerically the effect of Zeeman splitting on $R_{xx}(B)$ (using an effective g factor of -0.44) due to which the two spin directions acquire different Fermi energies and therefore different partial conductances, resulting in a spin polarization of the current. Our simulations suggest that the influence of the spin splitting on $R_{xx}(B)$ is marginal. Also, it is found numerically that the spin polarization of the current increases with increasing barrier height in the closed regime, but is below 10^{-3} for all magnetic fields. However, this value is about a factor of 5 larger than the simulated values for magnetic barriers without edges, and we conclude that edge transmission tends to increase the spin polarization. Even accounting for this increase, the effect for a 2DEG in Ga[Al]As remains very small. Finally, we have also incorporated magnetic mass effects induced by the strong parallel magnetic field[33] and find that they are negligible in our parameter range.

V. SUMMARY AND CONCLUSION

We have studied the resistance of magnetic barriers defined in Ga[Al]As heterostructures in the quasiballistic regime as a function of in-plane magnetic fields. We have also described the system numerically within a semiclassical model, and we find that the finite resistance observed in the closed regime originates from both elastic scattering in the barrier region and from transmission via $E \times B$ drifts at the edges of the Hall bar. By using the scattering times as extracted from the experiment, a very good agreement between measurement and simulation is obtained, especially given the uncertainties involved regarding the exact shape and homogeneity of the magnetic barrier. Furthermore, the barrier magnetoresistance is insensitive to thermal smearing, spin polarization and magnetic mass effects. The results also

show how the resistance change induced by the magnetic barrier can be increased, which may be of importance if one wishes to observe quantum effects such as resonant tunneling[6] or spin polarization. First of all, both larger mobilities and Hall bars of reduced width will reduce the scattering in the barrier region and thereby increase the barrier resistance. Also, defining soft edges reduces in principle the transmission via $E \times B$ drift effects; our simulations however suggest that very soft edges with edge fields in the range of 100 V/m are required to obtain a noticeable effect. Finally, the deposition of clean ferromagnetic films under ultrahigh vacuum conditions should enhance the saturation magnetization almost up to a factor of 2 in our samples.

Our model can easily be extended to describe more complicated magnetic barrier structures, for example, those suggested recently for use as tunable spin filters.[8,11–15]

ACKNOWLEDGMENTS

The authors acknowledge the careful reading of the paper by Matthew Jenkins, stimulating discussions with Hengyi Xu as well as financial support by the *Heinrich-Heine-Universität Düsseldorf*.

*Electronic address: thomas.heinzel@uni-duesseldorf.de

[1] P. D. Ye, D. Weiss, R. R. Gerhardts, M. Seeger, K. von Klitzing, K. Eberl, and H. Nickel, Phys. Rev. Lett. **74**, 3013 (1995).
[2] A. Nogaret, D. N. Lawton, D. K. Maude, J. C. Portal, and M. Henini, Phys. Rev. B **67**, 165317 (2003).
[3] F. M. Peeters and X. Q. Li, Appl. Phys. Lett. **72**, 572 (1998).
[4] K. S. Novoselov, A. K. Geim, S. V. Dubonos, Y. G. Cornelissens, F. M. Peeters, and J. C. Maan, Phys. Rev. B **65**, 233312 (2002).
[5] F. M. Peeters and A. Matulis, Phys. Rev. B **48**, 15166 (1993).
[6] A. Matulis, F. M. Peeters, and P. Vasilopoulos, Phys. Rev. Lett. **72**, 1518 (1994).
[7] A. Majumdar, Phys. Rev. B **54**, 11911 (1996).
[8] Y. Guo, B.-L. Gu, Z. Zeng, J.-Z. Yu, and Y. Kawazoe, Phys. Rev. B **62**, 2635 (2000).
[9] G. Papp and F. M. Peeters, Appl. Phys. Lett. **78**, 2184 (2001).
[10] G. Papp and F. M. Peeters, Appl. Phys. Lett. **79**, 3198 (2001).
[11] H. Z. Xu and Y. Okada, Appl. Phys. Lett. **79**, 3119 (2001).
[12] Y. Guo, Z. Feng, B.-L. Gu, and Y. Kawazoe, Phys. Rev. B **66**, 045312 (2002).
[13] Y. Jiang, M. B. A. Jalil, and T. Low, Appl. Phys. Lett. **80**, 1673 (2002).
[14] F. Zhai and H. Q. Xu, Phys. Rev. B **72**, 085314 (2005).
[15] F. Zhai and H. Q. Xu, Appl. Phys. Lett. **88**, 032502 (2006).
[16] M. L. Leadbeater, C. L. Foden, J. H. Burroughes, M. Pepper, T. M. Burke, L. L. Wang, M. P. Grimshaw, and D. A. Ritchie, Phys. Rev. B **52**, R8629 (1995).
[17] I. S. Ibrahim, V. A. Schweigert, and F. M. Peeters, Phys. Rev. B **56**, 7508 (1997).
[18] F. G. Monzon, M. Johnson, and M. L. Roukes, Appl. Phys. Lett. **71**, 3087 (1997).
[19] V. Kubrak, A. C. Neumann, B. L. Gallagher, P. C. Main, and M. Henini, J. Appl. Phys. **87**, 5986 (2000).
[20] T. Vančura, T. Ihn, S. Broderick, K. Ensslin, W. Wegscheider, and M. Bichler, Phys. Rev. B **62**, 5074 (2000).
[21] V. Kubrak, K. W. Edmonds, A. C. Neumann, B. L. Gallagher, P. C. Main, M. Henini, C. H. Marrows, B. J. Hickey, and S. Thoms, IEEE Trans. Magn. **37**, 1992 (2001).
[22] B. L. Gallagher, V. Kubrak, A. W. Rushforth, A. C. Neumann, K. W. Edmonds, P. C. Main, M. Henini, C. H. Marrows, B. J. Hickey, and S. Thoms, Physica E (Amsterdam) **11**, 171 (2001).
[23] J. Hong, V. Kubrak, K. W. Edmonds, A. C. Neumann, B. L. Gallagher, P. C. Main, M. Henini, C. H. Marrows, B. J. Hickey, and S. Thoms, Physica E (Amsterdam) **12**, 229 (2002).
[24] M.-W. Lu, L.-D. Zhang, and X.-H. Yan, Phys. Rev. B **66**, 224412 (2002).
[25] W. Xu and Y. Guo, Phys. Lett. A **340**, 281 (2005).
[26] D. R. Behrendt, S. Legvold, and F. H. Spedding, Phys. Rev. **109**, 1544 (1958).
[27] V. Stepankin, Physica B **211**, 345 (1995).
[28] M. Büttiker, Phys. Rev. Lett. **57**, 1761 (1986).
[29] C. W. J. Beenakker and H. van Houten, Phys. Rev. Lett. **63**, 1857 (1989).
[30] The heterostructures have been purchased from Intelligent Epitaxy Tech., Richardson, TX (USA).
[31] T. Ando, A. B. Fowler, and F. Stern, Rev. Mod. Phys. **54**, 437 (1982).
[32] P. A. Lee and T. V. Ramakrishnan, Rev. Mod. Phys. **57**, 287 (1985).
[33] S. K. Bhattacharya, Phys. Rev. B **25**, 3756 (1982).
[34] M. Johnson, B. R. Bennett, M. J. Yang, M. M. Miller, and B. V. Shanabrook, Appl. Phys. Lett. **71**, 974 (1997).
[35] J. Reijniers and F. M. Peeters, Appl. Phys. Lett. **73**, 357 (1998).
[36] J. Reijniers and F. M. Peeters, J. Appl. Phys. **87**, 8088 (2000).
[37] S. Liu, H. Guillou, A. D. Kent, G. W. Stupian, and M. S. Leung, J. Appl. Phys. **83**, 6161 (1998).
[38] Y. G. Cornelissens and F. M. Peeters, J. Appl. Phys. **92**, 2006 (2002).
[39] J. P. Harrang, R. J. Higgins, R. K. Goodall, P. R. Jay, M. Laviron, and P. Delescluse, Phys. Rev. B **32**, 8126 (1985).
[40] A. Fuhrer, S. Lüscher, T. Heinzel, K. Ensslin, W. Wegscheider, and M. Bichler, Phys. Rev. B **63**, 125309 (2001).
[41] I. A. Larkin and J. H. Davies, Phys. Rev. B **52**, R5535 (1995).